Biochimica et Biophysica Acta 1838 (2014) 1362–1371

Contents lists available at ScienceDirect

Biochimica et Biophysica Acta

journal homepage: www.elsevier.com/locate/bbamem

VDAC electronics: 1. VDAC-hexo(gluco)kinase generator of the mitochondrial outer membrane potential

Victor V. Lemeshko *

Escuela de Física, Facultad de Ciencias, Universidad Nacional de Colombia, sede Medellín, Calle 59A, No 63-20, Medellín, Colombia

ARTICLE INFO

Article history:
Received 31 August 2013
Received in revised form 25 December 2013
Accepted 1 January 2014
Available online 9 January 2014

Keywords:
VDAC
Hexokinase
Cancer
Aerobic glycolysis
Mitochondrial outer membrane potential
Computational model

ABSTRACT

The simplest mechanism of the generation of the mitochondrial outer membrane potential (OMP) by the VDAC (voltage-dependent anion channel)-hexokinase complex (VHC), suggested earlier, and by the VDAC-glucokinase complex (VGC), was computationally analyzed. Even at less than 4% of VDACs bound to hexokinase, the calculated OMP is high enough to trigger the electrical closure of VDACs beyond the complexes at threshold concentrations of glucose. These results confirmed our previous hypothesis that the Warburg effect is caused by the electrical closure of VDACs, leading to global restriction of the outer membrane permeability coupled to aerobic glycolysis. The model showed that the inhibition of the conductance and/or an increase in the voltage sensitivity of a relatively small fraction of VDACs by factors like tubulin potentiate the electrical closure of the remaining free VDACs. The extrusion of calcium ions from the mitochondrial intermembrane space by the generated OMP, positive inside, might increase cancer cell resistance to death. Within the VGC model, the known effect of induction of ATP release from mitochondria by accumulated glucose-6-phosphate in pancreatic beta cells might result not only of the known effect of GK dissociation from the VDAC-GK complex, but also of a decrease in the free energy of glucokinase reaction, leading to the OMP decrease and VDAC opening. We suggest that the VDAC-mediated electrical control of the mitochondrial outer membrane permeability, dependent on metabolic conditions, is a fundamental physiological mechanism of global regulation of mitochondrial functions and of cell death.
© 2014 Elsevier B.V. All rights reserved.

1. Introduction

VDAC, the most abundant protein of the mitochondrial outer membrane (MOM[1]) [1–4], is universally accepted as responsible for the control of metabolite fluxes between mitochondria and the cytosol [3–7]. This porin has been demonstrated to directly relate to many physiological processes and pathologies [5,7–9]. VDAC has even been considered as a governator of global mitochondrial functions both in health and disease [5]. However, experimental results related to the VDAC-mediated regulation of the MOM permeability and of cell death are confusing and contradictory, and the mechanisms responsible for this regulation remain poorly understood [4,10–12].

Although VDAC's electrical properties have been studied in detail [1–4,10,13], it has been generally considered as a permanently open pore under physiological conditions. Meanwhile, a large body of literature has been accumulated showing that VDAC conductance in living cells should be regulated [4,5,8–10,12–15]. It has been widely assumed that the MOM permeability is controlled by a partial or complete blockage of VDAC by various cytosolic proteins like tubulin [13–19], or in general, by various anti- and pro-apoptotic factors [5,7,8,10,12]. Many cases of apparently anomalous behavior of mitochondria and of global suppression of mitochondrial functions have been attributed to such reversible blockage-type regulation of the MOM permeability [5].

On the other hand, it is unlikely, according to Mannella et al. [20], that VDAC simply converts the MOM in a coarse sieve. We could add in this respect, that it is unlikely that the permeability of this sieve is simply regulated by only "molecular corks", as by hexokinase (HK) bound to VDAC, for example [21]. Meanwhile, the role of VDAC's highly conserved voltage gating properties remains to be the main unresolved question [4]. This question seems to be fundamental and can be answered possibly by finding the missing players of the MOM permeability regulation.

Earlier, we have proposed several steady-state mechanisms of the generation of metabolically-dependent OMP to demonstrate that the electrical closure-opening of VDAC might represent a physiological mechanism of regulation of the MOM permeability [22–24]. Experimental evidence of the generation of the negative OMP in living cells has been obtained by Porcelli et al. [25], although it is not yet clear, to

Abbreviations: VDAC, voltage-dependent anion channel; HK, hexokinase: GK, glucokinase; VHC, VDAC-HK complex; VGC, VDAC-GK complex; MIMS, mitochondrial intermembrane space; MOM, mitochondrial outer membrane; OMP, outer membrane potential; IMP, inner membrane potential; ANT, adenine nucleotide translocator; N_H, the percentage of VDACs bound to HK or to GK; N_{VS}, the percentages of voltage sensitive VDACs; N_{NS}, the percentage of voltage non-sensitive VDACs, TE, tubulin-like effectors; N_{TE}, the percentage of VDACs bound to TE; N_I, the percentage of VDACs completely blocked by an inhibitor

* Tel.: +57 4 4309378; fax: +57 4 4309327.
E-mail address: vvasilie@unal.edu.co.

0005-2736/$ – see front matter © 2014 Elsevier B.V. All rights reserved.
http://dx.doi.org/10.1016/j.bbamem.2014.01.001

what extent the metabolically-dependent inner membrane surface potential influenced the reported data, as it has been analyzed earlier [26].

According to one of the possible mechanisms of OMP generation, suggested earlier, the inner membrane potential (IMP) might be partly applied to the MOM through the intermembrane contact sites composed of adenine nucleotide translocator (ANT) and VDAC [23,24]. The same idea has recently been expressed by Pedersen [9]. In cancer cells, in addition, the resistance of the ANT-VDAC-HK contact sites has been suggested to decrease due to the free energy of the HK reaction applied to the contact sites, thus increasing the OMP [23,24]. The possible explanation of the Warburg effect has been proposed on the basis of global electrical closure of VDACs beyond the contact sites, due to the generated OMP. A similar concept has been developed in the last years by other authors [5,27], although without pointing to the electrical character of the MOM permeability suppression in cancer cells.

The simplest of the proposed mechanisms of the OMP generation has been based on the VDAC-HK complex only [23,24], because, for example, the mitochondrial intermembrane contact sites have not been found in the subpopulation HT29 Glc^+ of adenocarcinoma cells, although HK was predominantly bound to mitochondria [28]. Computational analysis of this model could represent certain interest for understanding possible mechanisms of the regulation of aerobic glycolysis and cell death. It has been discovered that in cancer cells, a large proportion of HK is associated with mitochondria [29,30 and reference therein] that has also been found to increase cancer cell resistance to death [8,9,11,12,31,32]. In addition, cancer cells have been characterized by a high rate of aerobic glycolysis and by a mitochondrial HK activity up to more than two orders of magnitude higher than in normal cells [33,34]. It has been found that both the HK binding to VDAC and the glucose phosphorylation reaction contribute to the protective effects of HK-I and HK-II against cell death [35]. It might be related to a decrease of the calcium concentration in the MIMS due to the positive OMP generation by VHC, according to the physical principles described earlier [23,24].

In the present work, we developed the VHC and VGC models of generation of the OMP, with the Gibbs free energy of kinase reactions as a driving force, as a battery in an equivalent electrical circuit. The calculations showed that the OMP value directly depends on the percentage of VDACs bound to HK, on the glucose concentration, and on the presence of tubulin-like effectors (TE). The calculated OMPs were high enough to electrically close VDAC. The positive sign of the OMP generated by the VHC might explain a high resistance of cancer cells to death as a result of calcium extrusion from the mitochondrial intermembrane space (MIMS). The model can be applied to pancreatic beta cells, for mitochondria of which high values of the OMP were calculated using the VGC model. Development and computational analysis of such and similar models seems to be an important approach to the further understanding of cell energy metabolism regulation, as well as of many cases of apparently anomalous behavior of mitochondria reviewed and analyzed in detail in [5].

2. Materials and methods

2.1. The VDAC-hexokinase complex model

According to the VHC model shown in Fig. 1A, ATP from the MIMS and glucose from the cytoplasm are used by HK bound to VDAC in the MOM, liberating ADP back into the MIMS and producing cytoplasmic glucose-6-phosphate. 100% of all VDACs in the MOM can be expressed as the sum of the percentage of VDACs bound to HK (N_H), of the percentages of the voltage sensitive VDACs (N_{VS}), and of voltage non-sensitive VDACs (N_{NS}), as well as of the percentage of VDACs bound to tubulin-like effectors (TE) influencing VDAC voltage sensitivity and/or partially blocking it (N_{TE}), and even of the percentage of

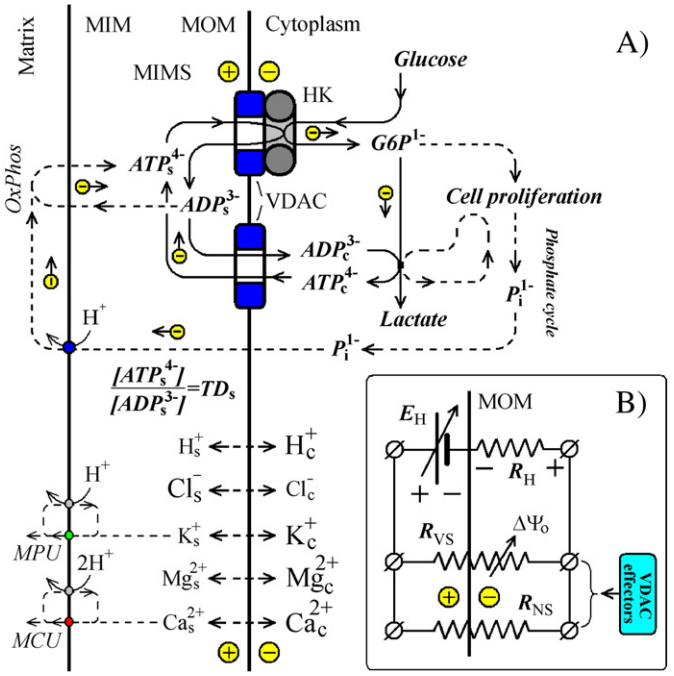

Fig. 1. The main principle of the OMP generation by the VDAC-hexokinase complex. A — VHC functioning leads to a charge separation across the MOM. The generated potential leads to the free VDAC closure strongly restricting ADP release from the MIMS to recover ATP in the cytoplasm. It represents the suggested anti-turbo mechanism of regulation of aerobic glycolysis allowing usage of mitochondrial ATP for the first stage of glycolysis in cancer cells (dotted lines). Ions H^+, Cl^-, K^+, Mg^{2+}, Ca^{2+} permeate through free VDACs in the MOM, achieving their electrochemical equilibrium. MPU — mitochondrial potassium uniporter; MCU — mitochondrial calcium uniporter. B — An equivalent electrical circuit of the VHC model: the battery E_H represents Gibbs free energy of the hexokinase reaction. The battery internal resistance, R_H, depends on the percentage of VDACs bound to HK. The resistance of the fraction of free voltage non-sensitive VDACs (as low sensitive VDAC3, for example) is presented as the resistance R_{NS} connected in parallel to the resistance R_{VS} of the remaining voltage gating VDACs. According to Ohm's law, the OMP generation results from voltage division on the equivalent resistance of free VDACs (R_{NS} and R_{VS}), that might be influenced by various VDAC effectors, and on the internal resistance of the battery R_H. Note, as the VDACs begin to close, their increasing resistance leads to further OMP increase by the mechanism of positive feedback control, allowing the MOM permeability regulation that depends on the glucose concentration and on the $[ATP]_s/[ADP]_s$ ratio.

VDACs completely blocked by some inhibitors (N_I):

$$100 = N_H + N_{VS} + N_{NS} + N_{TE} + N_I \quad (1)$$

The conductance g_{NS} (resistance $R_{NS} = 1/g_{NS}$ in Fig. 1B) of the N_{NS} fraction is not affected by the OMP, thus we can write $g_{NS} = N_{NS}$, expressing conductance in arbitrary units, a.u. The maximum conductance of the MOM was taken as 100 a.u., for 100% of all VDACs in the open state.

The conductance g_{VS} (resistance R_{VS} in Fig. 1B) of the fraction N_{VS} can be expressed as the function of the OMP ($\Delta\psi_o$) using an equation similar to that published earlier [22–24], at an arbitrary voltage-sensitivity parameter "*S1*":

$$g_{VS} = N_{VS} \cdot P_{c1} + N_{VS} \cdot (1 - P_{c1}) \cdot \exp\left(-(S1 \cdot \Delta\psi_o s)^2\right). \quad (2)$$

We used here $S1 = 40\ V^{-1}$ allowing almost complete VDAC closure at $\Delta\psi_o = \pm 40$ mV, as shown in Fig. 2a and b. The parameter P_{c1} is the VDAC relative conductance in the closed state, which was set in the range of 0.25–0.50 for various calculations [15,36–38].

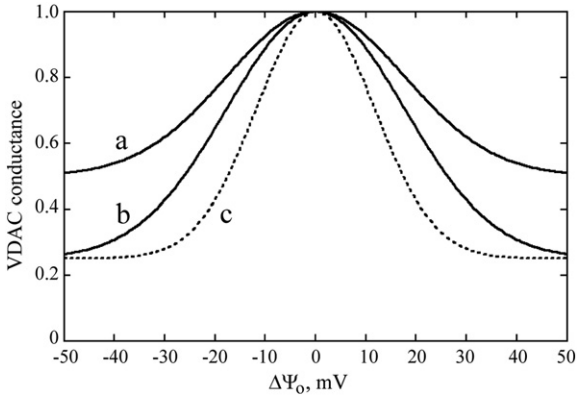

Fig. 2. The VDAC voltage-conductance characteristics. *a* — VDAC's typical voltage gating sensitivity allowing almost complete VDAC closure at ±40 mV, S1 = 40 V^{-1} and P_{c1} = 0.50 in Eq. (2); *b* — the same as *a*, but at P_{c1} = 0.25; *c* — the same as *b*, but at S2 = 60 V^{-1} (not used for calculations).

As tubulin has been shown to increase the voltage sensitivity of VDAC [15,19], the conductance g_T of the fraction N_{TE} can be presented as:

$$g_T = N_{TE} \cdot P_{c2} + N_{TE} \cdot (1 - P_{c2}) \cdot \exp\left(-(S2 \cdot \Delta\psi_o)^2\right). \quad (3)$$

The resting VDAC conductance in the presence of TE was set at $P_{c2} = 0.25$, instead of $P_{c1} = 0.5$ in the control, thus allowing an increase in the VDAC voltage sensitivity according to [15]. The model also allows an additional mechanism of an increase in voltage sensitivity, through an increase in the parameter *S2*, as shown in Fig. 2c for $S2 = 60\ V^{-1}$ in comparison with $S2 = 40\ V^{-1}$ (Fig. 2b).

The total conductance g_V of the MOM, as the sum of conductances of unbound VDACs (N_{VS}, N_{NS}) and of the fraction bound to TE (N_T) can be expressed as:

$$g_V = g_{VS} + g_{NS} + g_T \quad (4)$$

The influence of the glucose concentration in the cytoplasm, $[Gluc]_c$, on the conductance g_H of the fraction N_H of VDACs (VHCs) means a change of the internal resistance R_H ($R_H = 1/g_H$) of the battery E_H (Fig. 1B). The normalized hyperbolic factor with the Michaelis–Menten constant for glucose, $K_{m,G} = 0.1$ mM, was included. We assumed, for the sake of the simplicity, that the MIMS concentration of ATP is not a limiting factor for the rate of the HK reaction. The model also allows a consideration that the conductance, g_H at the maximum rate of the HK reaction is less than that of free VDAC by a factor K. Finally, g_H was expressed as:

$$g_H = \frac{N_H \cdot K \cdot [Gluc]_c}{K_{m,G} + [Gluc]_c} \quad (5)$$

The VHC functions as an electrogenic carrier of one negative net charge through the membrane, leading to the OMP generation, as shown in Fig. 1A. At no leakage of charged metabolites of the reaction through the membrane, the system would stay at equilibrium and the generated membrane potential would have maximum value, $\Delta\psi_{max}$, that can be directly related to the Gibbs free energy of the HK reaction:

$$\Delta\psi_{max,H} = -\left(\frac{\Delta G_H^{o'}}{F} + \frac{RT}{F} \ln \frac{[G6P]_c \cdot [ADP]_s}{[Gluc]_c \cdot [ATP]_s}\right). \quad (6)$$

Here, *F* is the Faraday constant, *R* is the universal gas constant, $T = 310\ K$ is normal body temperature, $[G6P]_c$ and $[Gluc]_c$ are concentrations of glucose-6-phosphate and glucose, respectively, in the cytoplasm, and $[ADP]_s$ and $[ATP]_s$ are concentrations of ADP and ATP in the MIMS. For most of the calculations, we used fixed $[G6P]_c = 0.1$ mM, i.e. in the reported normal physiological range. For the circuit shown in Fig. 1B, the voltage, E_H of the battery is equal to $\Delta\psi_{max,H}$. At $\Delta G_H^{o'} = -16.7$ kJ/mol, $E_H{}^{o'} = 173$ mV.

In the case of a leakage, $g_V \neq 0$ (permanent movement of a net charge of cycling metabolites trough free VDACs), the OMP ($\Delta\psi_o$) can be expressed as:

$$\Delta\psi_o = \frac{\Delta\psi_{max,H} \cdot g_H}{g_V + g_H} \quad (7)$$

This is according to Ohm's law, applied to the circuit in Fig. 1B. At $g_V = 0$, we have $\Delta\psi_o = \Delta\psi_{max}$. The VHC current, as an indicator of the HK activity of VHC, can be presented as:

$$I_h = \Delta\psi_o \cdot gV \quad (8)$$

At steady-state generated OMP, the permeable ions X^z, as H^+, Cl^-, K^+, Ca^{2+}, Mg^{2+}, etc., will stay at electrochemical equilibrium and will be distributed across the MOM according to the Nernst equation:

$$\Delta\psi_o = \frac{RT}{zF} \ln \frac{[X^z]_c}{[X^z]_s} m, \quad (9)$$

Here, $[X^z]_c$ and $[X^z]_s$ are ion concentrations in the cytoplasm and in the MIMS, respectively, *z* is the ion valence. The calculations were made for only calcium ions.

According to the Goldman's equation, the ATP flux (J_T) through the MOM at given conductance g_V and ATP concentrations in the MIMS and the cytoplasm ($[ATP]_s$ and $[ATP]_c$, respectively) should also depend on the calculated $\Delta\psi_o$:

$$J_T = -g_V \cdot \frac{\Delta\psi_o \cdot zF}{RT} \cdot \frac{[ATP]_s - [ATP]_c \cdot \exp\left(\frac{-\Delta\psi_o \cdot zF}{RT}\right)}{1 - \exp\left(\frac{-\Delta\psi_o \cdot zF}{RT}\right)} \quad (10)$$

Here, *F* is the Faraday constant, *R* is the universal gas constant, $T = 310\ K$ is normal body temperature, and *z* is the ATP valence (−4). Similarly, for the ADP flux (J_D):

$$J_D = -g_V \cdot \frac{\Delta\psi_o \cdot zF}{RT} \cdot \frac{[ADP]_s - [ADP]_c \cdot \exp\left(\frac{-\Delta\psi_o \cdot zF}{RT}\right)}{1 - \exp\left(\frac{-\Delta\psi_o \cdot zF}{RT}\right)}. \quad (11)$$

Here, $[ADP]_s$ and $[ADP]_c$ are ADP concentrations in the MIMS and the cytosol, respectively, and *z* is the ADP valence (−3).

2.2. The VDAC-glucokinase complex model

The VGC model is the same as VHC (Fig. 1), with the same Gibbs free energy of the kinase reaction. The system of the same Eqs. (1)–(9) was used to describe the VGC model, with one exception that the Michaelis–Menten constant for glucose in this case is higher, $K_{m,G} = 7.5$ mM, that is known to be near the regulated level of glucose concentration in human beta cells.

The calculations were made by numerical methods using the licensed software Mathcad Professional 2001i (MathSoft, Cambridge, MA).

3. Results

The VHC model was analyzed at various hypothetical metabolic conditions and depending on the percentages of VDACs bound to HK (N_H), of free VDACs (voltage sensitive, N_{VS}, and insensitive, N_{NS}), of

VDACs bound to the effectors like tubulin, N_{TE}, and of VDACs completely blocked by some inhibitor, N_I.

The calculated OMPs ($\Delta\psi_o$) for the physiological range of glucose concentrations at the fixed $[ATP]_s/[ADP]_s$ ratio in the MIMS (TDs = 200, as for example 10 mM ATP and 0.05 mM ADP) are shown in Fig. 3A. In the case of $N_{NS} = 0$ and the absence of VDAC inhibitors ($N_I = 0$), a well-expressed sigmoid increase in the OMP was revealed at different threshold concentrations of glucose, depending on the resting conductance P_{c1} (Eq. (2)) of VDAC in the closed state and on the percentage of VDACs bound to HK (Fig. 3A, curve a for $P_{c1} = 0.35$, $N_H = 4.0$, and Fig. 3A, curve b for $P_{c1} = 0.30$, $N_H = 3.5$). A sharp stepwise increase in the OMP was revealed when $P_{c1} = 0.25$ was used for calculations (Fig. 3A, curve c for $P_{c1} = 0.25$, $N_H = 3.0$). These calculations allowed demonstration that the character of VDAC switching might be regulated by a change of P_{c1}, if it is possible. High OMPs were also calculated for $P_{c1} = 0.4$ at $N_H = 4.2$ (Fig. 3C, a), and for $P_{c1} = 0.5$ at $N_H = 5.0$ (Fig. 3C, a).

A sharp character of an increase in the OMP at $P_{c1} = 0.25$ and $N_H = 3.4$ (Fig. 3B, a) was converted to a sigmoid curve when the fraction of voltage-insensitive VDACs ($N_{NS} = 5$, Eq. (1)) was also included in the system (Fig. 3B, b). At $N_{NS} = 10$, it was converted to an almost linear function (Fig. 3B, c). A significantly lower potential was calculated even in this case if the voltage gating was switched off by taking $S1 = 0$, Eq. 2 (Fig. 3B, d). All these calculations (Fig. 3) were made assuming K = 1 (Eq. (5)).

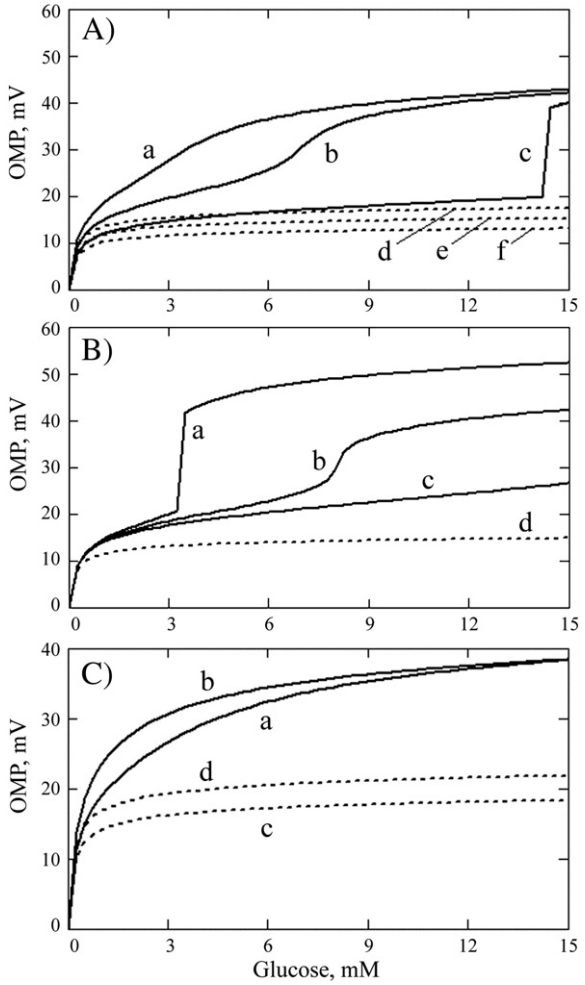

Fig. 3. Sigmoid characters of the generation of high OMPs at threshold concentrations of glucose. The calculations were made at TDs = 200 ([ATP]/[ADP] ratio in the MIMS), $S1 = 40\ V^{-1}$ and $N_I = 0$. Panel A – at $N_{NS} = 0$: *a* – $P_{c1} = 0.35$, $N_H = 4.0$; *b* – $P_{c1} = 0.30$ and $N_H = 3.5$; *c* – $P_{c1} = 0.25$, $N_H = 3.0$; Dotted lines – the switched off voltage gating, $S1 = 0\ V^{-1}$, for: *d* – $P_{c1} = 0.35$, $N_H = 4.0$; *e* – $P_{c1} = 0.30$ and $N_H = 3.5$; *f* – $P_{c1} = 0.25$, $N_H = 3.0$. Panel B – at $P_{c1} = 0.25$, $N_H = 3.4$: *a* – $N_{NS} = 0$; *b* $N_{NS} = 5$; *c* – $N_{NS} = 10$; *d* – the switched off voltage gating, $S1 = 0\ V^{-1}$, for the case *c*. Panel C: *a* – at $P_{c1} = 0.4$ and $N_H = 4.2$; *b* – at $P_{c1} = 0.5$ and $N_H = 5.0$; *d* and *c* – the switched off voltage gating, $S1 = 0\ V^{-1}$, for the cases *a* and *b*, respectively.

Very similar results were obtained considering, for example, that at the maximum rate of the HK reaction, the VHC conductance is 10 times lower (K = 0.1) than that of free VDAC (Fig. 4B, a), at TDs = 20, $P_{c1} = 0.25$, $N_{NS} = 5$. For comparison, OMPs calculated at K = 1 under the same conditions are shown in Fig. 4A, a. In the case of K = 0.1, a higher percentage of VHC was needed (32% instead of 4.2%) to generate relatively high OMPs. Significantly lower potentials were calculated at S1 = 0 (Eq. (2)) for both K = 1 and K = 0.1 (Fig. 4A and B, respectively, curves b). The OMP-dependent decrease in g_V was revealed at increasing concentrations of glucose for both K = 1 (Fig. 4C, a) and for K = 0.1 (Fig. 4D, a). The calculations for switched off voltage gating, $S1 = 0\ V^{-1}$, are presented in Fig. 4C and D, respectively, curves c). On the other hand, the potential-dependent decrease in the HK activity of VHCs was not markedly expressed, although detected for both K = 1 (Fig. 4C, b and d, for $S1 = 40\ V^{-1}$ and $S1 = 0\ V^{-1}$, respectively) and K = 0.1 (Fig. 4D, b and d, for $S1 = 40\ V^{-1}$ and $S1 = 0\ V^{-1}$, respectively).

For the sake of the simplicity of the model, the above mentioned calculations (Fig. 4A–D) were made without consideration of the OMP influence on the individual steady-state fluxes of ATP and ADP. But separately, Goldman's equation was applied taking into account the OMP calculations presented in Fig. 4A,B, for an arbitrary condition of relatively higher concentrations of ATP and ADP in the MIMS than in the cytosol: $[ATP]_s = 20$ mM, $[ADP]_s = 1$ mM (TDs = 20), and $[ATP]_c = 10$ mM, $[ADP]_c = 0.02$ mM ($TD_c = 500$). The calculations made demonstrated the complete block of ADP release from mitochondria by generated OMPs at glucose concentrations higher than 4 mM for K = 1 (Fig. 4E), and higher than 3 mM for K = 0.1 (Fig. 4F). A significantly smaller effect of the OMPs was revealed for the ATP influx (Fig. 4, G and H, for K = 1 and K = 0.1, respectively) that might exceed the ADP flux (Fig. 4, E and F, for K = 1 and K = 0.1, respectively) by two orders of magnitude, if steady-state conditions of 1ATP/1ADP exchange are not maintained.

The behavior of the VHC model under variation of the $[ATP]_s/[ADP]_s$ ratio in the MIMS (TD_s) and of the glucose concentration in the cytoplasm was estimated for two options: at the absence of the fraction of voltage-insensitive VDACs ($N_{NS} = 0$) at $N_H = 3.4$, $P_{c1} = 0.25$ (Fig. 5A,C,E,G) and for the presence of the N_{NS} fraction of VDACs ($N_{NS} = 5$) at $N_H = 3.4$, $P_{c1} = 0.25$ (Fig. 5B,D,F,H). The OMP values ($\Delta\psi_o$), the MOM permeability (g_V), and the VHC current (I_h), as well as the concentration of calcium ions in the MIMS ($[Ca^{2+}]_i$), were calculated. A sharp stepwise increase in $\Delta\psi_o$ at the threshold values of glucose concentration and/or of the critical values of TD_s was revealed at $N_H = 3.4$, $P_{c1} = 0.25$ and $N_{NS} = 0$ conditions (Fig. 5A). On the other hand, the model did not predict high values of $\Delta\psi_o$ at very low TD_s (less than 30) in the scanned range of glucose concentrations, or at relatively small glucose concentrations (less than 3 mM) in the scanned range of TD_s (Fig. 5A).

As a result of the sharp stepwise character of $\Delta\psi_o$ increase, the MOM permeability was also decreased abruptly, up to the final level somewhat less than 25% (Fig. 4C), determined by $P_{c1} = 0.25$ for the VDAC closed state, and by $N_H = 3.4$ excluded from 100% of VDACs. Interestingly, the VHC HK activity, expressed as the VHC current I_h, was restricted very slightly, although well detected (Fig. 5E). Another consequence of the generation of the positive potential $\Delta\psi_o$ was a decrease of the calcium ion concentration in the MIMS, by up to two orders of magnitude (Fig. 4G). Marked decrease in the MIMS calcium concentration was also revealed without VDAC closure (Fig. 5G), only due to a voltage drop on the resistance of the open state VDACs, according to the circuit shown in Fig. 1B and to Ohm's law.

In the presence of the 5% fraction of the voltage-insensitive, permanently open VDACs ($N_{NS} = 5$), higher threshold concentrations of

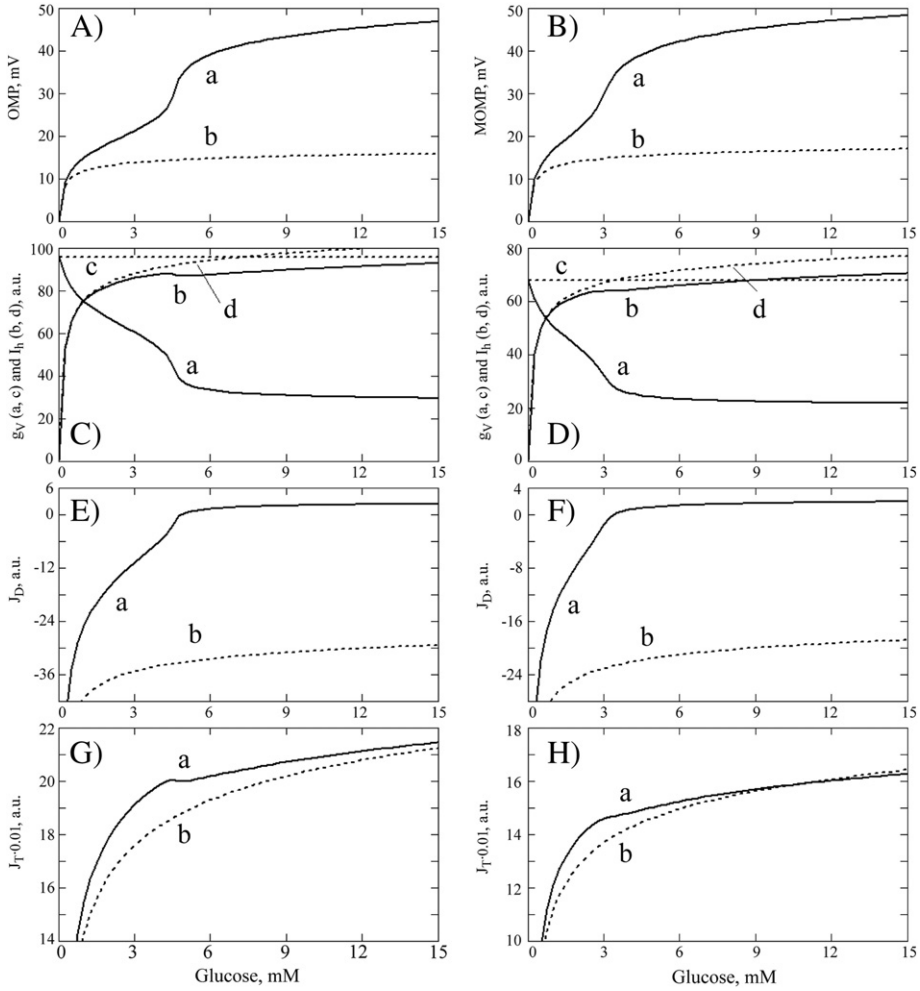

Fig. 4. Glucose concentration-dependent VHC-mediated generation of the OMP (A,B) and the closure of free VDACs (C,D, curves a,c) coupled to the VHC hexokinase activity (C,D, curves b,d), affecting ADP release from the MIMS (E,H) and ATP entrance into the MIMS (G,H). Left column — K = 1, N_H = 4.2 (Eq. (5)); Right column — K = 0.1, N_H = 32 (Eq. (5)). The calculations were made at TDs = 20, P_{c1} = 0.25 and N_{NS} = 5. Dotted lines — the switched off voltage gating, S1 = 0 V^{-1}, Eq. 2. The ADP and ATP fluxes were calculated according to Goldman's equation for arbitrary fixed conditions: $[ATP]_c$ = 10 mM, $[ADP]_c$ = 0.02 mM (TD_c = 500), and $[ATP]_s$ = 20 mM, $[ADP]_s$ = 1 mM (TDs = 20).

cytoplasmic glucose and higher values of TD_s were needed to trigger free, voltage-sensitive VDACs to the closed state, according to the generated OMP (Fig. 5B), and hence to suppress the MOM permeability even at relatively high TD_s (Fig. 5D). On the other hand, the VHC current was restricted very slightly (Fig. 5F). The decrease in the MIMS concentration of calcium ions in this case was by almost 1.5 orders of magnitude (Fig. 5H). High OMPs were calculated at the increased percentage of the VHC complexes (N_H = 4.2) even at N_{NS} = 10 (OMPs higher than shown in Fig. 4B) in the same range of changes of glucose concentration and/or TD_s ratios (calculations not shown).

Tubulin and many other cytoplasmic proteins were reported as physiological modulators of the MOM permeability by targeting VDAC and by restricting its conductance in the closed state [13–19] thus increasing the voltage sensitivity of VDAC [15,19]. Here we analyzed the VHC model at TE quantities up to N_{TE} = 50 (Fig. 6). Other parameters of the model were fixed at: TD_s = 200, N_H = 4.4, $S1$ = 40 V^{-1}, $S2$ = 40 V^{-1}, P_{c1} = 0.50 and P_{c2} = 0.25. According to the calculations, an increase in the TE percentage leads to a remarkable increase in OMP (Fig. 6B) and to the additional restriction of MOM permeability (Fig. 6E) due to the process of electrical closure of VDACs. At VDAC's voltage sensitivity parameters set to zero ($S1$ = 0 V^{-1}, $S2$ = 0 V^{-1}), the presence of TE at any concentration does not influence the OMP (Fig. 6A) or the MOM permeability (Fig. 6D).

Higher values of the OMP were calculated, if in addition to the mentioned effects of TE, some inhibitor targets VDAC, completely blocking 10% of VDACs (Fig. 6C), thus causing additional restriction of the MOM permeability (Fig. 6E).

The VGC model, in comparison to the VHC model, is characterized by lower affinity of glucokinase to glucose ($K_{m,G}$ = 7.5 mM, in Eq. (5)). Fixing parameters of the model at N_{NS} = 5, TD_s = 200, N_H = 7, $S1$ = 40 V^{-1} and P_{c1} = 0.25 (Eq. (2)), the calculations made demonstrated that at small concentrations of glucose-6-phosphate, as 0.1 mM, very high OMPs can be generated at glucose concentrations higher than 6 mM (Fig. 7A), leading to a strong restriction of the MOM permeability (Fig. 7B). On the other hand, at a high fixed glucose concentration, as 12 mM for example, an increase in the glucose-6-phosphate concentration leads to the reopening of free VDACs and to a significant increase in the MOM permeability (Fig. 7B), as a result of the OMP decrease (Fig. 7A,C).

Under the conditions of 12 mM glucose and 0.1 mM glucose-6-phosphate, the OMP potential was increased as a sigmoid function of the percentage of VGC (of VDACs bound to GK), with a mid-point near 5% VGC (Fig. 7C, a). Significantly lower, linear increase of the OMP was revealed at $S1$ = 0 V^{-1} (Fig. 7C), as a result of voltage drop on the resistance of the open VDACs. Applying Goldman's Eq. (10) for an arbitrary condition of 20 mM ATP in the MIMS and 5 mM ATP in the cytoplasm, it was determined that even at 3.3% VGC, when VDACs are almost

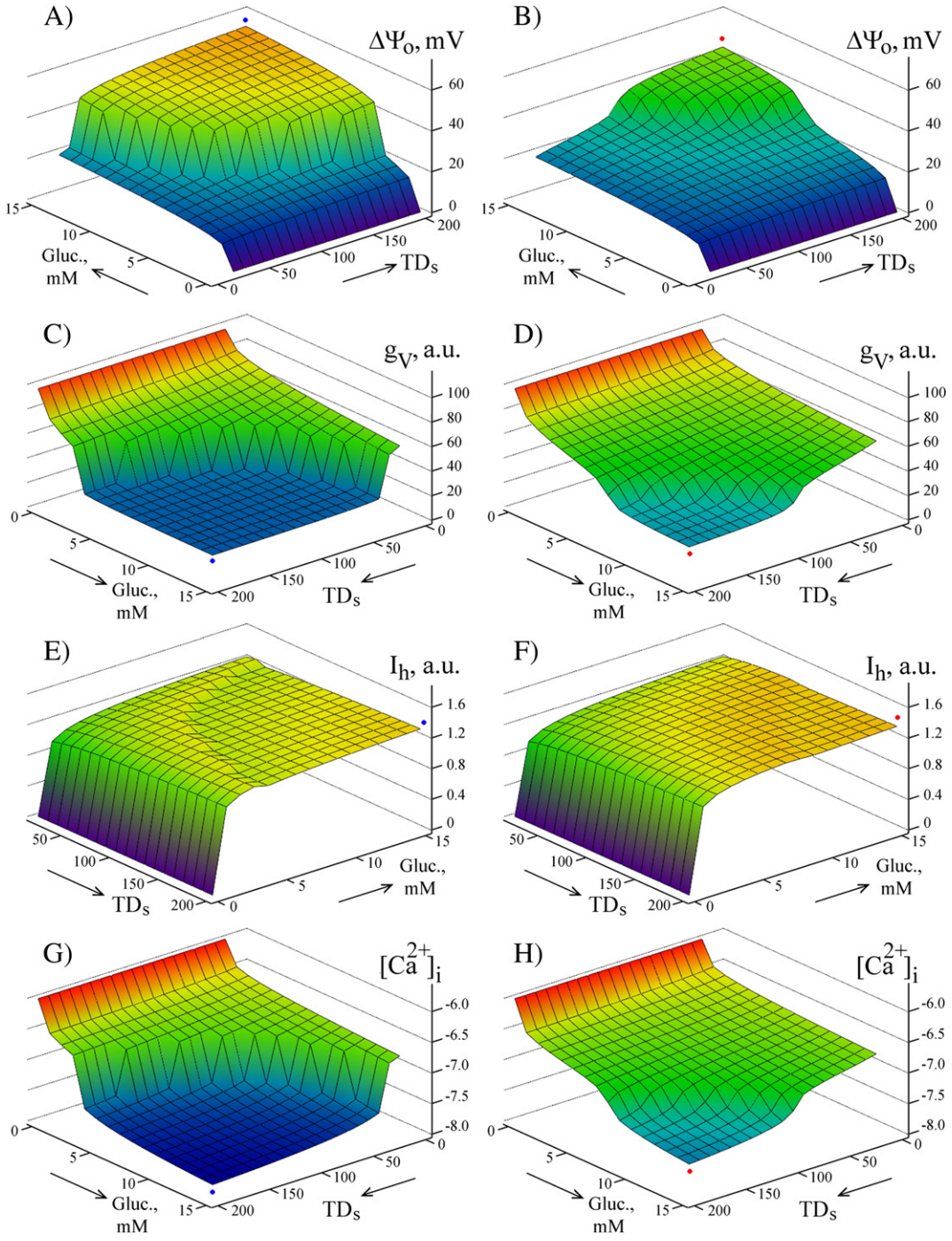

Fig. 5. The dependence of the VHC-generated OMP ($\Delta\psi_o$) (A,B), of the MOM conductance g_V (C,D) and of the calcium extrusion from the MIMS (G,H) coupled to the VHC hexokinase activity I_h (E,F) on the glucose concentration and on the ratio $[ATP]_s/[ADP]_s$ (TD_s), at $K = 1$, $P_{c1} = 0.25$, $N_H = 3.4$ (Eq. (5)). Left column — $N_{NS} = 0$; Right column — $N_{NS} = 5$.

completely open, the ATP flux was still directed from the cytoplasm to the MIMS (Fig. 7D, $S1 = 40\ V^{-1}$, positive ATP flux). It was decreased to a level of zero by switching off the voltage gating of VDAC (Fig. 7D, $S1 = 0\ V^{-1}$).

When the concentration of glucose-6phosphate was increased to 10 mM, it significantly increased ATP release at 3.3% VGC, shifting the zero flux-points to 4.2% and 4.5%, for $S1 = 40\ V^{-1}$ and $S1 = 0\ V^{-1}$, respectively (Fig. 7D,C). Further acceleration of ATP release in the presence of 10 mM glucose-6-phosphate, when all VDACs are open, might be achieved due to the dissociation of GK from the VDAC-GK complex, thus decreasing VGC% (Fig. 7C,D).

The presented calculations clearly showed high probability of the generation of the OMP by the VDAC-HK and VDAC-GK complexes in the MOM, allowing electrical suppression of mitochondria and efficient calcium extrusion from the MIMS.

4. Discussion

The electrical mechanism of VDAC closure, as a physiological regulation of VDAC conductance, is not yet widely accepted [4]. Generation of the metabolically-derived OMPs in living cells has been generally considered doubtful. The reason for such doubts is that even in the closed

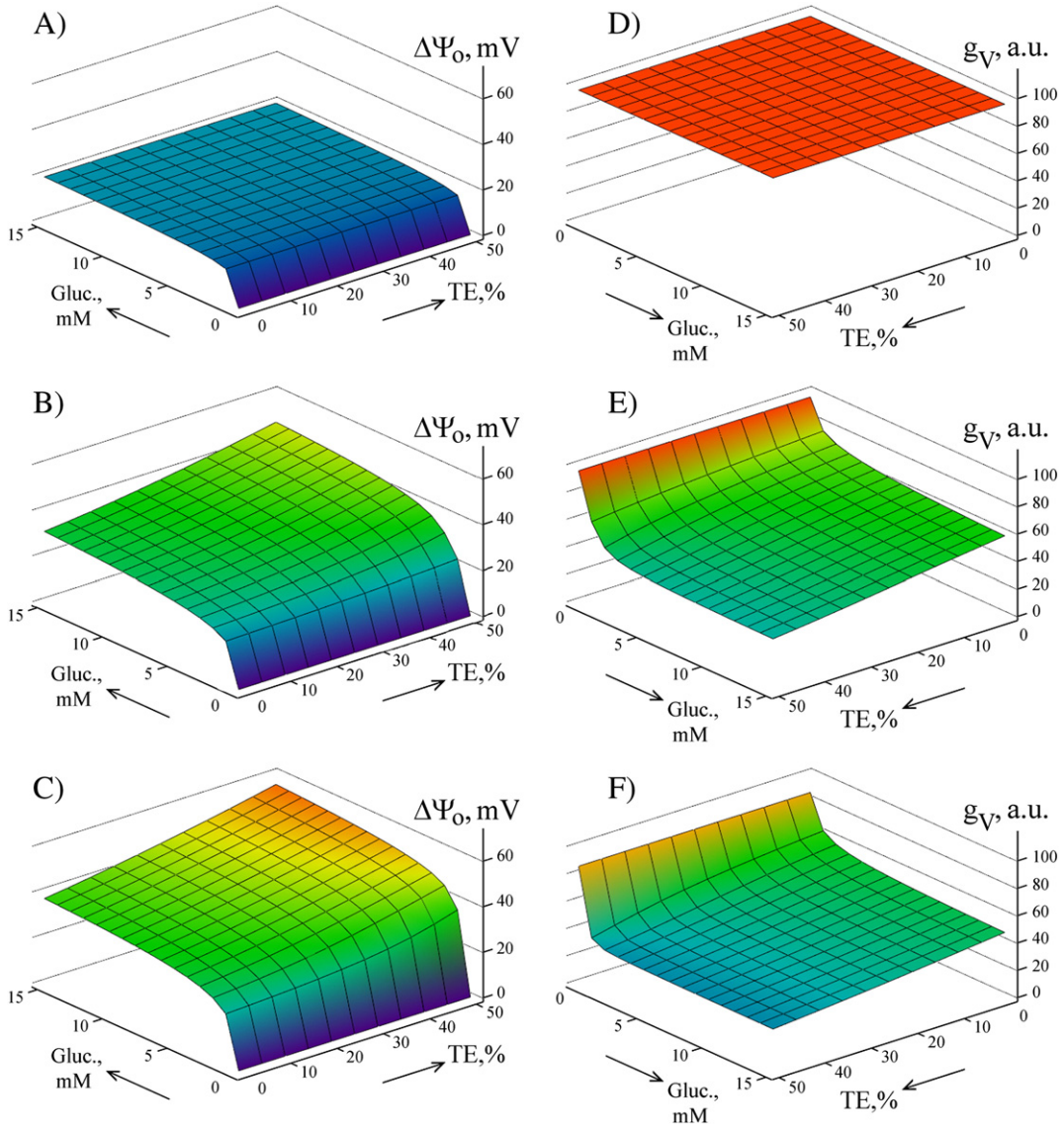

Fig. 6. Possible effects of tubulin-like VDAC effectors (TE) on the VHC-dependent OMP generation (A–C) and on the MOM conductance g_V (D–F). The calculations were made at $N_H = 4.4$, $P_{c1} = 0.50$, $P_{c2} = 0.25$ and $TD_s = 200$. A, D — controls, at $S1 = 0\ V^{-1}$, $S2 = 0\ V^{-1}$); B, E — at $S1 = 40\ V^{-1}$, $S2 = 40\ V^{-1}$; C, F — in addition to B and E, some inhibitor blocks 10% of VDACs ($N_I = 10$).

state VDAC conducts small ions, like K^+, Na^+, Ca^{2+}, which are believed to tend to collapse electrical potentials forming across the MOM [5,14]. Electrodynamic compartmentation of various permeable ions and possible osmotic effects caused by a steady-state generated OMP have been analyzed in our previous publications [22,24]. However, permeable ions that do not constantly circulate through the MOM should achieve their electrochemical equilibrium in accordance with the OMP generated by some steady-state mechanism. After that, they should not influence the steady-state generated membrane potential.

For comparison, the resting potential of excitable cells are normally calculated using complete form of the GHK equation, containing K^+, Na^+ and Cl^- terms. However, a simplified form of the GHK equation is often used in most biological studies [39], ignoring the Cl^- term, although the membrane permeability for Cl^- through chloride channels might be one order of magnitudes higher than that for Na^+. The simplified GHK equation is acceptable if the membrane is passively permeable to Cl^-, and thus Cl^- ions are not a part of the Na/K steady-state mechanism of the resting potential generation. The Cl^- equilibrium potential is frequently close to the resting potential [39–42], when the resting potential sets the Cl^- gradient rather than vice versa.

In this work, we developed the simplest steady-state models of generation of the OMP, based on the Gibbs free energy of kinases bound to VDAC, specifically hexokinase (VHC model) and glucokinase (VGC model). The models allowed computational analysis of a possible range of membrane potentials that could be supported by the Gibbs free energy of kinase reactions. The calculations obtained for the VHC model (Fig. 1), described by Eqs. 1–9, clearly demonstrated that HK bound to VDAC may be a very powerful generator of the OMP, as shown in Figs. 3–5. The calculated OMPs were high enough to electrically close the free voltage-sensitive VDACs even if we assume that the maximum HK reaction rate of VHC is 10 times less than the conductance of unbound VDAC in the open state (Fig. 4B,D). The effect of the possible presence of a fraction of voltage-insensitive VDACs was also analyzed (Fig. 5), because up to 11% of all VDACs in the MOM has been reported to have low voltage sensitivity [18].

The VHC model showed that the MOM permeability can be strongly restricted as a result of an abrupt electrical closure of VDACs at the

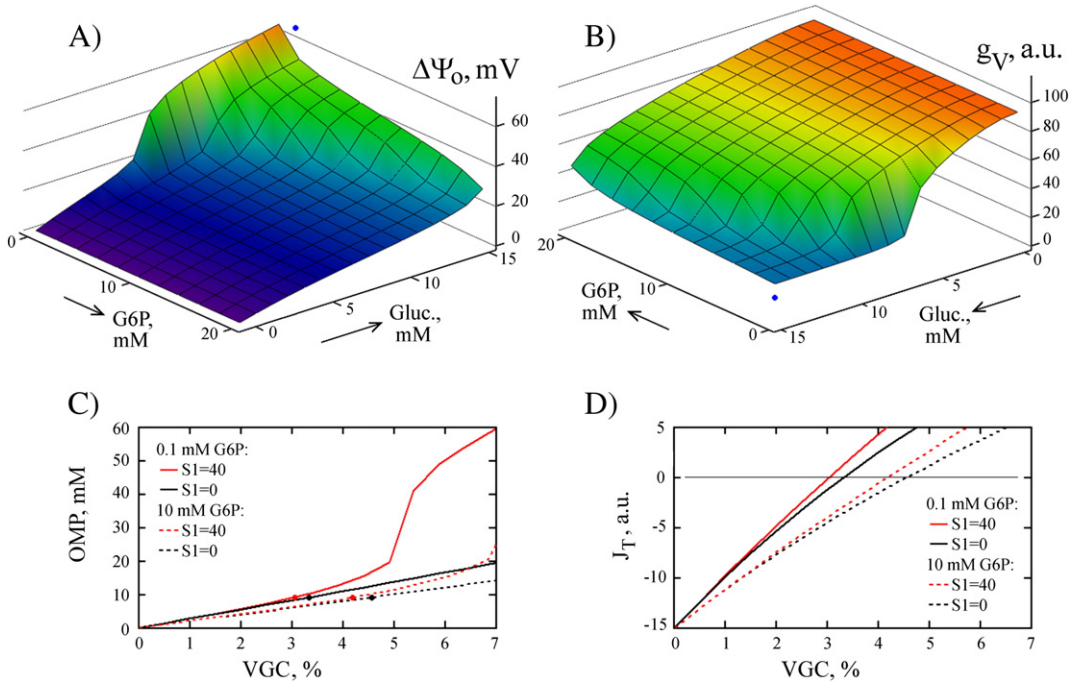

Fig. 7. VGC-mediated generation of the OMP (A) and the MOM conductance g_V changes (B), as the function of glucose and glucose-6-phosphate concentrations. The calculations were made at: $N_H = 7$, $S1 = 40\ V^{-1}$ and $P_{c1} = 0.25$ (Eq. (2)), $N_{NS} = 5$, $TD_s = 200$. C — the dependence of the OMP on the percentage of VDACs bound to GK (VGC) at 12 mM glucose and at the 0.1 mM and 10 mM concentrations of glucose-6phosphate. D — ATP flux through the MOM calculated according to the Goldman's equation for arbitrary fixed conditions: 20 mM ATP in the MIMS and 5 mM ATP in the cytoplasm (negative values correspond to ATP release).

threshold concentrations of glucose and/or the $[ATP]_s/[ADP]_s$ ratios. The threshold values depended on the percentage of VDACs bound to HK (Figs. 3 and 5). Both glucose concentration and the $[ATP]_s/[ADP]_s$ ratio influence the Gibbs free energy of the HK reaction (Eq. (6)). In the equivalent electrical circuit, the free energy is presented as a battery with the voltage E_H (Fig. 1B) according to Eq. (6). The calculations showed that VDAC electrical closure depends on metabolic conditions and should also depend on factors influencing the rate of the HK reaction of VHC (thus affecting the internal resistance R_H of the battery E_H).

Interestingly, even a significant restriction of the MOM permeability only slightly influenced the HK reaction rate of VHC (Fig. 4C,D, curves b, and Fig. 5E). This is due to a high internal resistance R_H (i.e. of a small fraction of VHC, N_H) in comparison with that of free VDACs) (Fig. 1B). On the other hand, the generated OMPs (Fig. 4A,B, curves a) were high enough to strongly prevent ADP release from the MIMS (Fig. 4E,F, curves a) that should lead to inhibition of the HK reaction. The calculations made using Goldman's Eq. 10, in a.u., showed that the entrance of cytosolic ATP into the MIMS may be slightly increased in this case, in comparison with completely open VDACs (Fig. 4G,H, curves a and b, respectively). But, if we take into account a well known specific property of the closed VDAC, to be almost completely impermeable to ATP [43,44], the closure of VDACs (Fig. 4C,D, curves a) means a complete prevention of the use of cytoplasmic ATP by VHC and of the use of ADP from the MIMS to recover ATP in the cytosol.

The metabolic burst might develop, if cytosolic ATP is easily accessible for HK to initiate the first step of aerobic glycolysis, leading to a so-called "turbo effect" of the uncontrolled activation of glycolysis. That is why, in trypanosomes, the turbo-explosion seems to be prevented by the membrane separation of the first stage of glycolysis, by the glycosomal compartmentation of glycolysis [45–47]. In cancer cells, such a compartmentation might result from the HK binding to VDAC and from the OMP-dependent regulation of the MOM permeability to adenine nucleotides [23,24].

ADP accumulated in the MIMS can enter the mitochondrial matrix to recover ATP in the process of oxidative phosphorylation (Fig. 1A). The positive OMP favors this process by facilitating inorganic phosphate influx into the MIMS. Once in the MIMS, it is transported into the mitochondrial matrix by the known pH-dependent phosphate carrier. Hence, phosphate cycling (Fig. 1A) might decrease the steady-state generated OMP by some extent, but does not collapse it. This is because the resistance of the phosphate cycle seems to be relatively large, as it is composed of several resistances in series, namely of an equivalent resistances of cell proliferation, of phosphate transport through the inner membrane, of oxidative phosphorylation process, and of ATP/ADP exchange through the ANT, in addition to the resistance of the MOM. The limitation of inorganic phosphate has been reported as the major rate-limiting factor of glycolysis in Ehrlich ascites tumor cells [48], and as a factor partly reducing tumor cell respiration rate [49].

The MOM might also function as an electrical barrier to energy flux, due to the VDAC-mediated generation of the membrane potential. This electrical barrier might be additional to a physical barrier of the electrically closed VDACs per se. Both electrical and physical barriers result in highly effective suppression of a direct use of mitochondrially produced ATP in the cytoplasm. In this respect, the VHC-dependent generation of the OMPs, controlled by metabolic conditions, might represent a very effective anti-turbo mechanism of the regulation of aerobic glycolysis in cancer cells. Due to the OMP-dependent electro-diffusion barrier, this anti-turbo mechanism allows the restriction of the access of ADP produced in the MIMS to the cytoplasm, significantly diminishing the possibility of ATP recovery in the cytoplasm using mitochondrial ADP. At the same time, it should facilitate aerobic glycolysis using mitochondrial ATP by the mode dependent on the inorganic phosphate cycling coupled to the cytoplasmic use of glucose-6-phosphate for biosynthesis and cell growth (Fig. 1A) at a known restriction of phosphate entry into the cell [49].

Surprisingly, the mitochondrial HK activity of many cancer cells has been shown to be higher than in normal cells by two orders of magnitude [33,34]. In addition, the HK binding to mitochondria has been demonstrated to increase cell resistance to death [8,9,11,12,31,32,35]. The calculated OMPs, positive inside, should cause calcium extrusion from the MIMS, leading to a decrease of its concentration by up to two orders of magnitude (Fig. 5G,H) near the inner membrane calcium

uniporter (Fig. 1A). This mechanism should prevent calcium overload of mitochondria that might be the simplest explanation of high resistance to death of cells with an elevated quantity of HK bound to mitochondria [21,27,31,32,35], and of the dependence of the death-protective effect on the mitochondrial HK activity [35]. The final effect might be similar to that caused by an inhibition of the mitochondrial calcium uniporter [50]. In contrast to cancer cells, in which the calcium extrusion from the MIMS is expected (Fig. 5G,H) due to the positive OMP generation (Fig. 5A,B), the OMP in epithelial cells ECV304 in vitro has been reported to be negative and relatively high [25]. Hence, the negative OMP should favor calcium flux into mitochondria and apoptosis induction. It has been found that VDAC in the closed state is more permeable for calcium than in the open state [51], thus VDAC should not prevent calcium equilibrium distribution between the MIMS and the cytosol according to the generated OMP.

A possible influence of tubulin-like effectors, TE, was analyzed within the VHC model (Fig. 6). The obtained results demonstrated that an increase in the VDAC voltage sensitivity, due to the binding of TE and a decrease of the closed state VDAC conductance, caused an increased generation of the OMP and induced the electrical closure of free voltage-sensitive VDACs (Fig. 6C,F). It was notable that the blockage of 10% of VDACs by a hypothetical inhibitor (as it would be VDAC3 knockdown reported in [18]), essentially increased the OMP generated by the VHC (Fig. 6C,F).

On the basis of these calculations, we could propose an additional, or even an alternative explanation of the recently reported decrease of the IMP in HepG2 cells caused by free tubulin [17,18]. The inner membrane potential has been monitored using a potential-sensitive probe $TMRM^+$ accumulated in mitochondria [17,18]. Only hypothetically, it is possible that the reported data of fluorescence changes were at least partially resulting from the superposition of the negative IMP and of the positive OMP, thus leading to the underestimation of the IMP. Under the conditions described in Fig. 6B legend, for example, the calculated OMP, positive inside, was higher by approximately 30 mV at 85% TE in the range of 3–15 mM glucose concentrations (data not shown). Now, let us assume that the OMP = 0, IMP = −180 mV, and the $TMRM^+$ fluorescence is 100 a.u., corresponding to the 1000-fold gradient of $TMRM^+$ in the inner membrane (according to the Nernst equation). However, at OMP = 30 mV and the same IMP = −180 mV, the $TMRM^+$ fluorescence should be near 32 a.u., because the positive OMP should strongly decrease the $TMRM^+$ concentration in the MIMS. These results are in the range of the reported changes of the $TMRM^+$ fluorescence [17,18]. On the other hand, $TMRM^+$ uptake into the mitochondrial matrix might not be altered significantly if, in addition to the OMP generation, the IMP is also increased, due to the restriction of the MOM permeability to adenine nucleotides and/or a possible decrease of the delta pH component of the inner membrane proton motive force.

Thus, our "electrical" explanation might be applied to the mentioned experimental conditions [17,18] at least in addition to the functioning of tubulin as a "molecular cork" [14,17,18]. Although very low concentrations or even the absence of beta-2 tubulin have been suggested for many types of cancer cells [52], the tubulin-containing structures are important in any case for the formation of the mitotic spindles during mitosis [53]. In this respect, it has been reported that in the presence of a new drug MPT0B214, inhibiting tubulin polymerization, human carcinoma cells were arrested in the G_2-M phase, and the subsequent cell death has been attributed to the apoptosis associated with mitochondria-mediated intrinsic pathway [53].

Erastin, the selective anti-tumor agent, has been reported to be able to bound to VDAC2 [54], and to increase $TMRM^+$ fluorescence, with or without free tubulin [18]. These fluorescence changes might be related to a decrease of the OMP, positive inside, generated by VHC (Fig. 6), if erastin competes with both tubulin binding [18] and hexokinase binding to VDAC. A possible decrease of the OMP in the presence of erastin, as a result of the hexokinase detachment, might favor cancer cell death due to higher calcium concentrations in the MIMS (Fig. 5) in combination with oxidative stress induced by this drug [54].

In general, glucose deprivation, in addition to factors and conditions favoring HK dissociation from the VDAC-HK complex, should decrease cell resistance to death, especially if combined with drugs increasing cytosolic calcium concentration. Our VHC model allows the explanation of the Warburg effect as a result of the OMP-dependent electrical suppression of the outer membrane permeability [23,24]. Dissociation of HK from the VDAC-HK complex by 3-bromopyruvate [32] or by peptides derived from HK [12,55,56] or VDAC [8,57], especially in combination with the MOM permeabilizing factors [56], should cause the OMP collapse. Under such treatments, the drugs increasing cytoplasmic concentration of calcium ions [39] might favor cell death. This is concerned with a strategy of anticancer treatment focused on the VDAC-HK complex as a very important pharmacological target [5,7,9,27,55–57].

The computational analysis of the VGC model (that may be applied to mitochondria of pancreatic beta cells), showed that at more than 5% of VDAC bound to GK, the generated OMP values (Fig. 7A,C) might cause the electrical suppression of the MOM permeability (Fig. 7B). The calculations also showed that ATP retention in the MIMS might result from not only VDAC closure, but in addition, from the generated positive OMP, although not high enough to induce the VDAC closure (Fig. 7C,D). The calculations also demonstrated that an increase in the concentration of glucose-6-phosphate should potentiate ATP release from mitochondria even at high glucose concentrations. Further acceleration of ATP flux might be achieved by a decrease in the number of VDAC-GK complexes (Fig. 7C,D).

Glucose-6-phosphate accumulation in the cytosol has been reported as a factor inducing GK and HK dissociation from the VGC and VHC complexes [5,8,31,58]. Thus, the acceleration of the adenine nucleotide fluxes through the MOM by accumulated glucose-6-phosphate, to induce insulin secretion for example, might be a combined effect, the structural (VDAC-GK dissociation) and the thermodynamic (OMP decrease according to Eqs. 6 and 7), allowing temporary OMP decrease.

Downregulation of GK in pancreatic beta cells has been shown to decrease interactions between GK and mitochondria, leading to apoptosis [58]. According to our VGC model, a decrease in the OMP due to the GK detachment (decrease in VGC%, Fig. 7C) allowed higher concentrations of calcium in the MIMS (calculations not shown) that should contribute to the reported death induction [54] due to the activation of mitochondrial permeability transition pore [59]. In general, the VGC model of the OMP generation is consistent with the concept of the critical role of glucokinase in pancreatic beta cell metabolism and cell survival [60]. It is not yet clear, whether the potential-dependent distribution of permeable ions, such Ca^{2+}, Mg^{2+} and H^+ contribute to the process of binding/dissociation of GK to/from the VDAC. A significant effect of pH and Mg^{2+} concentration on HK binding to VDAC has been reported [29], but the influence of the OMP-dependent ion distribution between the MIMS and the cytosol has never been studied.

Conclusion. The presented models demonstrate the main principle of how the MOM permeability might be regulated by the electrical closure-opening of VDACs due to the OMP generation by one of the possible mechanisms described earlier [22–24], and by the VDAC-HK and VDAC-GK complexes analyzed here. Computational analysis of the suggested model strongly supports our earlier explanation of the Warburg effect as a result of the VDAC-mediated voltage-dependent restriction of the MOM permeability [23,24]. A similar explanation has been proposed by other authors, as a result of global mitochondrial suppression [5,14]. We believe that VDAC-mediated electrical regulation of mitochondrial suppression under some physiological conditions directly depends on hexo(gluco)kinase reactions, and thus on the metabolic conditions. It means that the MOM permeability might be regulated by the free energy of kinase reactions through the kinases bound to VDAC, by various regulatory factors and metabolic conditions.

Acknowledgments

The author thanks Dr. Sergy V. Lemeshko (St. Luke's Hospital, Houston, TX) for a productive discussion of the models and paper revision. Financial support for this work was provided by the Colciencias (Colombia) research grants #111852128625 and #5201-545-3156 (362-2011) and by the National University of Colombia, Medellin Branch.

References

[1] S.J. Schein, M. Colombini, A. Finkelstein, Reconstitution in planar lipid bilayers of a voltage-dependent anion-selective channel obtained from paramecium mitochondria, J. Membr. Biol. 30 (1976) 99–120.
[2] M. Colombini, A candidate for the permeability pathway of the outer mitochondrial membrane, Nature 279 (1979) 643–645.
[3] M. Colombini, VDAC structure, selectivity, and dynamics, Biochim. Biophys. Acta 1818 (2012) 1457–1465.
[4] M. Colombini, C.A. Mannella, VDAC, the early days, Biochim. Biophys. Acta 1818 (2012) 1438–1443.
[5] J.J. Lemasters, E. Holmuhamedov, Voltage-dependent anion channel (VDAC) as mitochondrial governator—thinking outside the box, Biochim. Biophys. Acta 1762 (2006) 181–190.
[6] D.G. Brdiczka, D.B. Zorov, S.S. Sheu, Mitochondrial contact sites: their role in energy metabolism and apoptosis, Biochim. Biophys. Acta 1762 (2006) 148–163.
[7] S. Fulda, L. Galluzzi, G. Kroemer, Targeting mitochondria for cancer therapy, Nat. Rev. Drug Discov. 9 (2010) 447–464.
[8] V. Shoshan-Barmatz, D. Mizrachi, VDAC1: from structure to cancer therapy, Front. Oncol. 2 (2012) 164.
[9] S.P. Mathupala, P.L. Pedersen, Voltage dependent anion channel-1 (VDAC-1) as an anti-cancer target, Cancer Biol. Ther. 9 (2010) 1053–1056.
[10] T.K. Rostovtseva, W. Tan, M. Colombini, On the role of VDAC in apoptosis: fact and fiction, J. Bioenerg. Biomembr. 37 (2005) 129–142.
[11] K.S. McCommis, C.P. Baines, The role of VDAC in cell death: friend or foe? Biochim. Biophys. Acta 1818 (2012) 1444–1450.
[12] J.G. Pastorino, J.B. Hoek, Regulation of hexokinase binding to VDAC, J. Bioenerg. Biomembr. 40 (2008) 171–182.
[13] T.K. Rostovtseva, B. Antonsson, M. Suzuki, R.J. Youle, M. Colombini, S.M. Bezrukov, Bid, but not Bax, regulates VDAC channels, J. Biol. Chem. 279 (2004) 13575–13583.
[14] E.N. Maldonado, J.J. Lemasters, Warburg revisited: regulation of mitochondrial metabolism by voltage-dependent anion channels in cancer cells, J. Pharmacol. Exp. Ther. 342 (2012) 637–641.
[15] T.K. Rostovtseva, S.M. Bezrukov, VDAC inhibition by tubulin and its physiological implications, Biochim. Biophys. Acta 1818 (2012) 1526–1535.
[16] A.V. Kuznetsov, S. Javadov, R. Guzun, M. Grimm, V. Saks, Cytoskeleton and regulation of mitochondrial function: the role of beta-tubulin II, Front. Physiol. 4 (2013) 82.
[17] E.N. Maldonado, J. Patnaik, M.R. Mullins, J.J. Lemasters, Free tubulin modulates mitochondrial membrane potential in cancer cells, Cancer Res. 70 (2010) 10192–10201.
[18] E.N. Maldonado, K.L. Sheldon, D.N. DeHart, J. Patnaik, Y. Manevich, D.M. Townsend, S.M. Bezrukov, T.K. Rostovtseva, J.J. Lemasters, Voltage-dependent anion channels modulate mitochondrial metabolism in cancer cells: regulation by free tubulin and erastin, J. Biol. Chem. 288 (2013) 11920–11929.
[19] T.K. Rostovtseva, S.M. Bezrukov, VDAC regulation: role of cytosolic proteins and mitochondrial lipids, J. Bioenerg. Biomembr. 40 (2008) 163–170.
[20] C.A. Mannella, M. Forte, M. Colombini, Toward the molecular structure of the mitochondrial channel, VDAC J. Bioenerg. Biomembr. 24 (1992) 7–19.
[21] C. Rosano, Molecular model of hexokinase binding to the outer mitochondrial membrane porin (VDAC1): implication for the design of new cancer therapies, Mitochondrion 11 (2011) 513–519.
[22] S.V. Lemeshko, V.V. Lemeshko, Metabolically derived potential on the outer membrane of mitochondria: a computational model, Biophys. J. 79 (2000) 2785–2800.
[23] V.V. Lemeshko, Model of the outer membrane potential generation by the inner membrane of mitochondria, Biophys. J. 82 (2002) 684–692.
[24] S.V. Lemeshko, V.V. Lemeshko, Energy flux modulation on the outer membrane of mitochondria by metabolically-derived potential, Mol. Cell. Biochem. 256–257 (2004) 127–139.
[25] A.M. Porcelli, A. Ghelli, C. Zanna, P. Pinton, R. Rizzuto, M. Rugolo, pH difference across the outer mitochondrial membrane measured with a green fluorescent protein mutant, Biochem. Biophys. Res. Commun. 326 (2005) 799–804.
[26] V.V. Lemeshko, Theoretical evaluation of a possible nature of the outer membrane potential of mitochondria, Eur. Biophys. J. 36 (2006) 57–66.
[27] S.P. Mathupala, Y.H. Ko, P.L. Pedersen, Hexokinase-2 bound to mitochondria: cancer's stygian link to the "Warburg Effect" and a pivotal target for effective therapy, Semin. Cancer Biol. 19 (2009) 17–24.
[28] C. Denis-Pouxviel, I. Riesinger, C. Buhler, D. Brdiczka, J.-C. Murat, Regulation of mitochondrial hexokinase in cultured HT 29 human cancer cells: an ultrastructural and biochemical study, Biochim. Biophys. Acta 902 (1987) 335–348.
[29] I.A. Rose, J.V. Warms, Mitochondrial hexokinase. Release, rebinding, and location, J. Biol. Chem. 242 (1967) 1635–1645.
[30] D.P. Kosow, I.A. Rose, Ascites tumor mitochondrial hexokinase II. Effect of binding on kinetic properties, J. Biol. Chem. 243 (1968) 3623–3630.
[31] H. Azoula-Zohar, A. Israelson, S. Abu-Hamad, V. Shoshan-Barmatz, In self-defence: hexokinase promotes VDAC closure and prevents mitochondria-mediated apoptotic cell death, Biochem. J. 377 (2004) 347–355.
[32] Z. Chen, H. Zhang, W. Lu, P. Huang, Role of mitochondria-associated hexokinase II in cancer cell death induced by 3-bromopyruvate, Biochim. Biophys. Acta 1787 (2009) 553–560.
[33] R.A. Nakashima, M.G. Paggi, L.J. Scott, P.L. Pedersen, Purification and characterization of a bindable form of mitochondrial bound hexokinase from the highly glycolytic AS-30D rat hepatoma cell line, Cancer Res. 48 (1988) 913–919.
[34] A. Marín-Hernández, S. Rodríguez-Enríquez, P.A. Vital-González, F.L. Flores-Rodríguez, M. Macías-Silva, M. Sosa-Garrocho, R. Moreno-Sánchez, Determining and understanding the control of glycolysis in fast-growth tumor cells. Flux control by an over-expressed but strongly product-inhibited hexokinase, FEBS J. 273 (2006) 1975–1988.
[35] L. Sun, S. Shukair, T.J. Naik, F. Moazed, H. Ardehali, Glucose phosphorylation and mitochondrial binding are required for the protective effects of hexokinases I and II, Mol. Cell. Biol. 28 (2008) 1007–1017.
[36] G. Báthori, I. Szabó, I. Schmehl, F. Tombola, A. Messina, V. De Pinto, M. Zoratti, Novel aspects of the electrophysiology of mitochondrial porin, Biochem. Biophys. Res. Commun. 243 (1998) 258–263.
[37] J. Banerjee, S. Ghosh, Interaction of mitochondrial voltage-dependent anion channel from rat brain with plasminogen protein leads to partial closure of the channel, Biochim. Biophys. Acta 1663 (2004) 6–8.
[38] N. Arbel, D. Ben-Hail, V. Shoshan-Barmatz, Mediation of the antiapoptotic activity of Bcl-xL protein upon interaction with VDAC1 protein, J. Biol. Chem. 287 (2012) 23152–23161.
[39] D.C. Chang, Dependence of cellular potential on ionic concentrations. Data supporting a modification of the constant field equation, Biophys. J. 43 (1983) 149–156.
[40] K. Staley, R. Smith, J. Schaack, C. Wilcox, T.J. Jentsch, Alteration of GABAA receptor function following gene transfer of the CLC-2 chloride channel, Neuron 17 (1996) 543–551.
[41] R. Tyzio, M. Minlebaev, S. Rheims, A. Ivanov, I. Jorquera, G.L. Holmes, Y. Zilberter, Y. Ben-Ari, R. Khazipov, Postnatal changes in somatic gamma-aminobutyric acid signalling in the rat hippocampus, Eur. J. Neurosci. 27 (2008) 2515–2528.
[42] I. Rinke, J. Artmann, V. Stein, ClC-2 voltage-gated channels constitute part of the background conductance and assist chloride extrusion, J. Neurosci. 30 (2010) 4776–4786.
[43] T. Rostovtseva, M. Colombini, ATP flux is controlled by a voltage-gated channel from the mitochondrial outer membrane, J. Biol. Chem. 271 (1996) 28006–28008.
[44] T. Rostovtseva, M. Colombini, VDAC channels mediate and gate the flow of ATP: implications for the regulation of mitochondrial function, Biophys. J. 72 (1997) 1954–1962.
[45] J.R. Haanstra, A. van Tuijl, P. Kessler, W. Reijnders, P.A. Michels, H.V. Westerhoff, M. Parsons, B.M. Bakker, Compartmentation prevents a lethal turbo-explosion of glycolysis in trypanosomes, Proc. Natl. Acad. Sci. U. S. A. 105 (2008) 17718–17723.
[46] M. Gualdron-López, M.H. Vapola, I.J. Miinalainen, J.K. Hiltunen, P.A. Michels, V.D. Antonenkov, Channel-forming activities in the glycosomal fraction from the bloodstream form of *Trypanosoma brucei*, PLoS One 7 (2012) e34530.
[47] B.M. Bakker, F.I. Mensonides, B. Teusink, P. van Hoek, P.A. Michels, H.V. Westerhoff, Compartmentation protects trypanosomes from the dangerous design of glycolysis, Proc. Natl. Acad. Sci. U. S. A. 97 (2000) 2087–2092.
[48] R. Wu, Control mechanisms of glycolysis in Ehrlich ascites tumor cells, J. Biol. Chem. 240 (1965) 2827–2832.
[49] D.H. Koobs, Phosphate mediation of the Crabtree and Pasteur effects, Science 178 (1972) 127–133.
[50] R.R. Arvizo, D.F. Moyano, S. Saha, M.A. Thompson, R. Bhattacharya, V.M. Rotello, Y.S. Prakash, P. Mukherjee, Probing novel roles of the mitochondrial uniporter in ovarian cancer cells using nanoparticles, J. Biol. Chem. 288 (2013) 17610–17618.
[51] W. Tan, M. Colombini, VDAC closure increases calcium ion flux, Biochim. Biophys. Acta 1768 (2007) 2510–2515.
[52] T. Kaambre, V. Chekulayev, I. Shevchuk, M. Karu-Varikmaa, N. Timohhina, K. Tepp, J. Bogovskaja, R. Kütner, V. Valvere, V. Saks, Metabolic control analysis of cellular respiration in situ in intraoperational samples of human breast cancer, J. Bioenerg. Biomembr. 44 (2012) 539–558.
[53] N.J. Chiang, C.I. Lin, J.P. Liou, C.C. Kuo, C.Y. Chang, L.T. Chen, J.Y. Chang, A novel synthetic microtubule inhibitor, MPT0B214 exhibits antitumor activity in human tumor cells through mitochondria-dependent intrinsic pathway, PLoS One 8 (2013) e58953.
[54] N. Yagoda, M. von Rechenberg, E. Zaganjor, A.J. Bauer, W.S. Yang, D.J. Fridman, A.J. Wolpaw, I. Smukste, J.M. Peltier, J.J. Boniface, R. Smith, S.L. Lessnick, S. Sahasrabudhe, B.R. Stockwell, RAS-RAF-MEK-dependent oxidative cell death involving voltage-dependent anion channels, Nature 447 (2007) 864–868.
[55] J.G. Pastorino, N. Shulga, J.B. Hoek, Mitochondrial binding of hexokinase II inhibits Bax-induced cytochrome c release and apoptosis, J. Biol. Chem. 277 (2002) 7610–7618.
[56] N. Shulga, R. Wilson-Smith, J.G. Pastorino, Hexokinase II detachment from the mitochondria potentiates cisplatin induced cytotoxicity through a caspase-2 dependent mechanism, Cell Cycle 8 (2009) 3355–3364.
[57] S. Abu-Hamad, H. Zaid, A. Israelson, E. Nahon, V. Shoshan-Barmatz, Hexokinase-I protection against apoptotic cell death is mediated via interaction with the voltage-dependent anion channel-1: mapping the site of binding, J. Biol. Chem. 283 (2008) 13482–13490.
[58] J.W. Lee, W.H. Kim, J.H. Lim, E.H. Song, J. Song, K.Y. Choi, M.H. Jung, Mitochondrial dysfunction: glucokinase downregulation lowers interaction of glucokinase with mitochondria, resulting in apoptosis of pancreatic beta-cells, Cell. Signal. 21 (2009) 69–78.
[59] P. Bernardi, The mitochondrial permeability transition pore: a mystery solved? Front. Physiol. 4 (2013) 95.
[60] S. Liu, T. Okada, A. Assmann, J. Soto, C.W. Liew, H. Bugger, O.S. Shirihai, E.D. Abel, R.N. Kulkarni, Insulin signaling regulates mitochondrial function in pancreatic beta-cells, PLoS One 4 (2009) e7983.